Enhanced Raman Scattering from Individual Semiconductor Nanocones and Nanowires

Linyou Cao,[1] Bahram Nabet,[1,2,3] and Jonathan E. Spanier[1,2,3,*]

[1]*Department of Materials Science and Engineering, Drexel University, 3141 Chestnut Street, Philadelphia Pennsylvania 19104, USA*
[2]*Department of Electrical and Computer Engineering, Drexel University, 3141 Chestnut Street, Philadelphia Pennsylvania 19104, USA*
[3]*A. J. Drexel Nanotechnology Institute, Drexel University, 3141 Chestnut Street, Philadelphia Pennsylvania 19104, USA*

(Received 30 November 2005; published 18 April 2006)

We report strong enhancement ($\sim 10^3$) of the spontaneous Raman scattering from individual silicon nanowires and nanocones as compared with bulk Si. The observed enhancement is diameter (d), excitation wavelength (λ_{laser}), and incident polarization state dependent, and is explained in terms of a resonant behavior involving incident electromagnetic radiation and the structural dielectric cross section. The variation of the Raman enhancement with d, λ_{laser}, and polarization is shown to be in good agreement with model calculations of scattering from an infinite dielectric cylinder.

DOI: 10.1103/PhysRevLett.96.157402 PACS numbers: 78.67.Lt, 42.25.Fx, 42.68.Mj, 78.30.Am

The phenomenon of strong, resonant, and local enhancement of visible electromagnetic (EM) radiation when incident on the surface of metallic particles and films resulting from surface plasmon resonances continues to attract significant attention for fundamental and applied interests alike. This includes, for example, optical-based and surface-enhanced Raman-scattering detection of chemical and biochemical analytes [1], and in novel photonic devices involving electromagnetically coupled metallic nanostructures [2]. However, the possibility of enhancement of EM radiation from semiconducting and insulating materials, particularly in silicon, is noteworthy for silicon-based optoelectronic applications owing to the potential for monolithically integrating photonic technology and semiconductor electronics [3]. Because radiative recombination of electron-hole pairs in bulk Si is rather inefficient, optical gain in Si has been achieved only by using nanocrystals [4] or via stimulated Raman scattering [5,6]. The latter approach relies on Raman gain at certain levels of incident power that are high enough to exceed the light loss in the medium [7]. Enhanced Raman scattering is expected to increase the cavity Q and lower the threshold power for Raman gain [8,9].

Raman scattering from dielectric particles exhibits strong resonant effects when the wavelength of an incident field is commensurate with that of an electromagnetic eigenmode of the particle, which depends on its size and on the refractive indices of the particle and the surrounding medium [10]. Such resonant excitation results in large internal fields [11], and thus leads to enhancement of absorption [12], of radiation pressure [13], and of elastic and inelastic scattering [14,15]. Such features are expected to be important in the development of ultrahigh-Q and ultralow-threshold lasers [16]. Reports of the effects of structural resonances on Raman scattering have been limited mainly to theoretical and experimental investigations of nondispersive microstructures [10,14,15], of nanoparticles prepared without control of shape and size [17,18], and of lithographically patterned and substrate-integrated structures [18,19].

Here we present a combined experimental and theoretical investigation of the effects of silicon nanowire (SiNW) and silicon nanocone (SiNC) diameter (d), laser-excitation wavelength (λ_{laser}), and the incident linear polarization state on the Raman-scattering (RS) efficiency; we find these enhancements per unit volume to increase with decreasing diameter, with a RS efficiency that approaches $\sim 10^3$ times that of bulk, single-crystalline Si (c-Si). These enhancements depend sensitively on the location of the laser excitation along the SiNC, i.e., the average value of d probed, and on λ_{laser}. The enhancements are modeled by simulating the scattering from an infinite dielectric cylinder. Close correspondence between our calculated and experimental results provides strong validation of the structural resonance as the mechanism for the observed enhancement.

Solid SiNCs were prepared by metal nanostructure-catalyzed chemical vapor deposition (CVD) as described elsewhere [20]. In addition, SiNWs of selected diameters were also prepared via metal-catalyzed CVD. Control of SiNC formation during growth enables the production of ~ 25 μm-long SiNCs possessing diameters that range from several microns at the base to less than 5 nm at the tip [20]. As-grown SiNCs and SiNWs were sonicated from the substrate into ethanol solution, and cast onto Ni electronic microscopy grids for Raman-scattering spectroscopy and scanning electron microscopy (SEM) analysis. Several laser-excitation wavelengths were used: a 514.5-nm Ar^+ (0.3 mW incident power), 632.8-nm HeNe (0.8 mW), and 785-nm diode (0.08 mW) focused to Gaussian widths of ~ 1.0 μm, ~ 1.2 μm, and ~ 1.5 μm, respectively. Unpolarized Raman scattering was dispersed using a Renishaw 1000 Raman spectrometer and collected with an air-cooled CCD array detector. RS was collected at room temperature (~ 300 K) from more than 20 individual SiNCs, from nine individual SiNWs ($\sim 130\,\text{nm} \lesssim d \lesssim \sim 1\,\mu\text{m}$) and from a bulk, single-crystalline Si(100)

wafer in the backscattering configuration with incident polarization perpendicular (TE) or parallel (TM) to the main axis of each SiNC and SiNW [Fig. 1(a)]. Spectra were collected from a number of locations from the base to near the tip of each SiNC, where the diffraction-limited spot size limited resolving of the placement of the incident beam to a location corresponding to a minimum diameter of ~250 nm. For each λ_{laser} and each nanostructure, the ratio of Stokes-to-anti-Stokes-scattered intensity was evaluated to ensure that no laser-induced heating occurred. All enhancements reported here are from a single SiNC and from nine SiNWs; the results from this SiNC presented here are representative of all SiNCs studied. Shown in Fig. 1(b) is a scanning electron microscopy image of the SiNC studied; the apex angle of this SiNC is ~0.12 rad.

For 632.8-nm excitation, the integrated intensity from a SiNC near its base is observed to be approximately twice as large as that for bulk *c*-Si. The intensity is seen to depend on the probing location from the base to the tip, with a nearly monotonic increase for decreasing diameter. With the laser beam incident on a location of the SiNC corresponding to $d \sim 250$ nm, the intensity is approximately 5 times larger than that for bulk *c*-Si. Values of the Raman enhancement per unit volume (*RE*), defined here as the ratio of Raman intensities from a unit volume of SiNW (or SiNC) to bulk silicon, were calculated from the measured spectra for each location based on the spot size and the complex refractive index of bulk *c*-Si at each wavelength [21] using the relation $RE \equiv [I_{nw}/V_{nw}]/[I_{bulk}/V_{bulk}]$. Here, I_{nw} denotes the measured Raman intensity for a SiNW or SiNC, I_{bulk} is that for bulk Si(100), and V_{nw} the volume of SiNW or SiNC probed. Though the increase in absolute intensity near the tip is modest, the corresponding *RE* is significant. As shown in Fig. 2, the measured intensities at selected diameters for both TM (open black triangles) and TE (open inverted blue triangles) for $\lambda_{laser} =$ 632.8 nm incident laser excitation corresponds to a *RE* that is as large as ~250–300 near the SiNC tip. Also shown in Fig. 2 are the *RE*s from individual SiNWs of selected diameters for TE (solid black inverted triangles) and TM (solid blue inverted triangles). Significantly, the SiNWs exhibit essentially the same *RE* as the corresponding locations of the SiNC possessing the same average diameter. Among the SiNWs investigated, the largest enhancement (~800) is seen for a 130-nm diameter SiNW. Small but reproducible differences in the Raman-scattering intensities for TM and TE are also observed. Finally, the Raman-scattered intensity is also highly sensitive to λ_{laser}. The *RE* results for TM, $\lambda_{laser} = 514.5$ nm and $\lambda_{laser} = 785$ nm are shown in Fig. 3 along with that for $\lambda_{laser} = 632.8$ nm for both SiNWs and the SiNC. For these values of λ_{laser}, the *RE* is largest for 785 nm, and smallest for 514.5 nm.

The observed increase in Raman-scattering intensity with decreasing diameter in this system suggests that the enhancements may be due to structural resonances in the local field similar to Mie scattering from dielectric spheres [22]. Here, we simulate the Raman scattering from our nanowires by calculating the elastic scattering of a linearly-polarized, monochromatic, visible-wavelength plane wave with an incident propagation vector $k \perp \hat{z}$ by an infinitely long dielectric cylinder in vacuum. Calculations were performed for incident electric or magnetic field vectors perpendicular to the long axis of the nanowire [Fig. 1(a)]. For focused laser-excitation with Gaussian spot diameter *w* incident on a SiNW of length $l \gg w$ this model is a reasonable approximation for modeling the scattering from an individual SiNW. Further, given that the variation in the diameter of the SiNC inves-

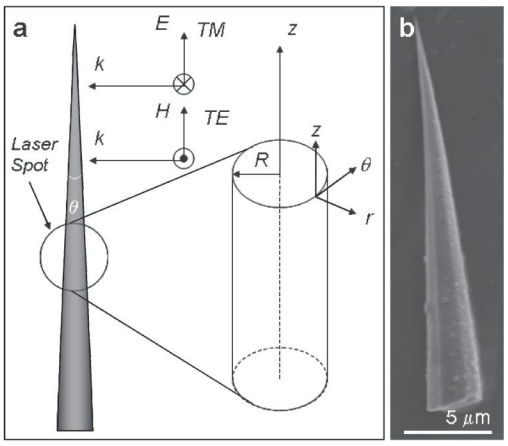

FIG. 1. (a) Schematic diagram of experimental configuration for Raman scattering from a silicon nanocone (SiNC) of diameter $d = 2R$ showing the direction of excitation laser incidence and of TE and TM fields. (b) Scanning electron micrograph of the individual SiNC used in this study.

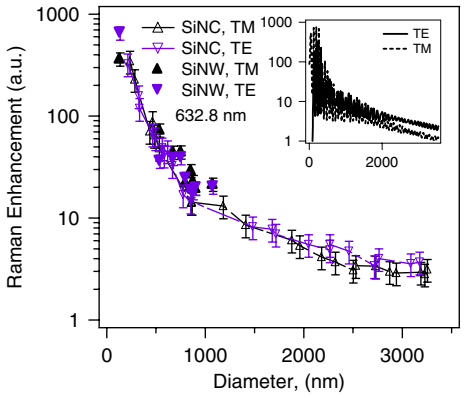

FIG. 2 (color online). Measured Raman enhancement (*RE*) for an individual silicon nanocone (open triangles) and a series of silicon nanowires (solid triangles) as functions of diameter for both TM-polarized (upright triangles) and TE-polarized (inverted triangles) 632.8-nm laser excitation as shown in the legend. Inset: calculated *RE*s as functions of diameter for 632.8-nm wavelength TE (solid) and TM (broken) polarized incident radiation. The experimental values of *RE* are determined from measured Raman-scattered intensities per unit volume of Si as described in the main text.

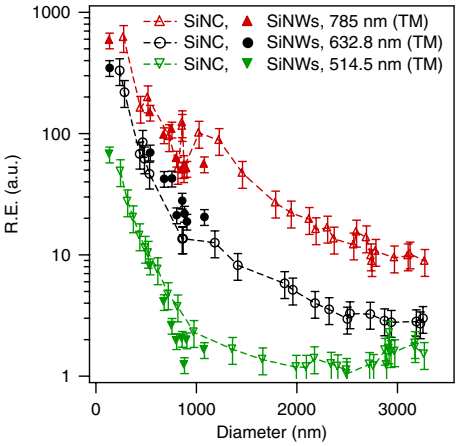

FIG. 3 (color online). Raman enhancements for a single silicon nanocone (open markers) at different locations and for individual silicon nanowires (solid markers). The data shown were collected using 785 (upright red triangles), 632.8 (black circles), and 514.5-nm (inverted green triangles), TM-polarized laser excitation.

tigated in this study varies ~100 nm over the incident laser spot size, we contend that it is also a reasonable approximation for modeling the scattering from a SiNC.

For incident radiation of frequency ω_0 spontaneous Raman scattering at the Raman-shifted frequency ω_1 can be described in terms of an incoherent summation over fields radiated from a distribution of induced polarization sources with strength proportional to the intensity of the local internal field. We model the scattering by solving Maxwell's equations and by applying the appropriate boundary conditions at the cylindrical vacuum-dielectric interface. The incident TE and TM plane wave field, and the internal and scattered fields are each expanded in cylindrical harmonics. This yields the internal electric fields [14]

$$E_{\text{int}}^{\text{TE}} = \frac{E_0}{k_1} \sum_{n=-\infty}^{\infty} (-i)^n c_n e^{in\theta} \left[\frac{in}{r} J_n(k_1 r)\hat{r} - k_1 J_n'(k_1 r)\hat{\theta} \right], \tag{1a}$$

$$E_{\text{int}}^{\text{TM}} = E_0 \sum_{n=-\infty}^{\infty} (-i)^n d_n J_n(k_1 r) e^{in\theta}\hat{z}, \tag{1b}$$

where E_0 is the amplitude of the incident electric field, k_1 $(=\omega(\varepsilon_1\mu_1)^{1/2})$ is the propagation constant in the nanowire, $J_n(k_1 r)$ is the cylindrical Bessel function of the first kind, and r is the distance from the center of the nanowire. The coefficients c_n and d_n can be related to far field scattering coefficients a_n and b_n by applying boundary conditions at the surface of the nanowire [14], yielding

$$c_n = \frac{J_n'(k_0 r) - a_n H_n'(k_0 r)}{J_n'(k_1 r)}, \tag{2a}$$

$$d_n = \frac{J_n(k_0 r) - b_n H_n(k_0 r)}{J_n(k_1 r)}, \tag{2b}$$

where k_0 is the propagation constant in the surrounding medium (vacuum) and $H_n(k_1 r)$ is the cylindrical Hankel function of the second kind. The far field scattering coefficients a_n and b_n are given by

$$a_n = \frac{J_n(k_0 r)J_n'(k_1 r) - mJ_n'(k_0 r)J_n(k_1 r)}{H_n(k_0 r)J_n'(k_1 r) - mH_n'(k_0 r)J_n(k_1 r)}, \tag{3a}$$

$$b_n = \frac{mJ_n(k_0 r)J_n'(k_1 r) - J_n'(k_0 r)J_n(k_1 r)}{mH_n(k_0 r)J_n'(k_1 r) - H_n'(k_0 r)J_n(k_1 r)}, \tag{3b}$$

where m is the refractive index of the cylinder, and k_0 is the propagation constant in air. The volume-averaged intensities of the internal field per unit length are obtained by integrating the squared field amplitudes [11]

$$\bar{I}_{\text{int}}^{\text{TE,TM}} = \frac{1}{\pi R^2} \int_0^R \int_0^{2\pi} |E_{\text{int}}^{\text{TE,TM}}|^2 r dr d\theta, \tag{4}$$

where R is the radius of the nanowire. Substituting Eq. (1) into Eq. (4), one obtains

$$\bar{I}_{\text{int}}^{\text{TE}} = \frac{E_0^2}{2} \sum_{n=-\infty}^{\infty} |c_n|^2 \{ J_{n-1}^2(k_1 R) + J_{n+1}^2(k_1 R) - J_n(k_1 R)[J_{n-2}(k_1 R) + J_{n+2}(k_1 R)] \}, \tag{5a}$$

$$\bar{I}_{\text{in}}^{\text{TM}} = E_0^2 \sum_{n=-\infty}^{\infty} |d_n|^2 [J_n^2(k_1 R) - J_{n-1}(k_1 R)J_{n+1}(k_1 R)]. \tag{5b}$$

Equations (5a) and (5b) describe the absolute intensity of the internal electric field in the nanowire. The diameter dependence is clear in this description. These being Bessel functions, they show oscillations which are also functions of R. Experimentally resolving this oscillatory behavior is useful in the general case of Mie scattering because it gives information about scatterer size. Of particular interest here is the ratio of this intensity in the nanowire to that in bulk single-crystalline Si, $Q_{\text{int}}^{\text{TE,TM}}(\omega_0) = \bar{I}_{\text{int}}^{\text{TE,TM}}/\bar{I}_{\alpha}^{\text{tra}}$, where the denominator denotes the average intensity within the dispersive medium. An enhanced internal field results in an increased polarization at a Raman-shifted frequency ω_1 and, therefore, to an increased inelastic scattering intensity. Since ω_1 and ω_0 differ here by less than 4% one can estimate that the scattered Raman field will also be enhanced by a factor $Q_s^{\text{TE,TM}}(\omega_1) \sim Q_{\text{int}}^{\text{TE,TM}}(\omega_0)$, and the total RE $Q_{\text{Raman}}^{\text{TE,TM}}$ can be approximated as $Q_{\text{Raman}}^{\text{TE,TM}} = Q_{\text{int}}^{\text{TE,TM}}(\omega_0)Q_s^{\text{TE,TM}}(\omega_1) \approx [Q_{\text{int}}^{\text{TE,TM}}(\omega_0)]^2$.

The calculated REs for TM for each of the three excitation wavelengths are plotted as functions of diameter in Fig. 4 along with the corresponding experimental results. The calculations are in good agreement with the measured decrease with diameter and increase with wavelength, though the simulated REs are consistently lower than those for the experimental data, and the experimental data do not exhibit the undulations with diameter that are seen in the simulated scattering even when considering the experimental error bars (see Figs. 2 and 3). We note that the experimentally observed difference in the TE and TM response (shown in Fig. 2) is also seen qualitatively in the calculated result of the inset of Fig. 2. The differences

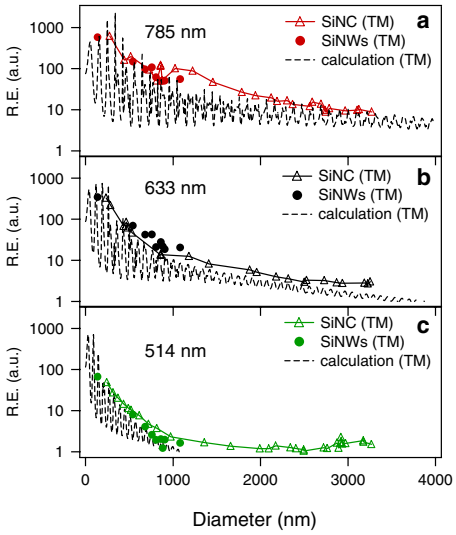

FIG. 4 (color online). Comparison of the simulated Raman enhancements based on infinitely long dielectric nanowires and those determined experimentally from a silicon nanocone (SiNC) and of a set of silicon nanowires (SiNWs) of selected diameters for (a) 785, (b) 632.8, and (c) 514.5-nm wavelength, TM-polarized laser excitation. The broken lines in each denote the simulation results, and the triangles and circles correspond to data for the SiNC and the SiNWs, respectively.

in Raman-scattered intensity among these laser-excitation wavelengths is in stark contrast to the λ^{-4} dependence that is expected for nonresonant Raman and elastic scattering processes, providing further evidence of a resonant nature of the observed scattering. The observed and calculated laser-excitation wavelength dependence of the *RE* for fixed diameter is influenced by the wavelength-dependent complex refractive index of silicon. Specifically, the values of *RE* for the model calculations and the experimental data can be plotted (not shown) as a function of normalized size $k_1 r$, where $k_1 = 2\pi m(\lambda)/\lambda$, $2r$ is the diameter, and $m(\lambda)$ is the real part of the index of refraction: the *RE* for small values of $k_1 r$ ($\lesssim 5$) for different wavelengths essentially collapse onto one trace, whereas for larger $k_1 r$ the different wavelength-dependent rates of decreases in the *RE* as a function of $k_1 r$ (and diameter at which *RE* approaches unity) are accounted for by the different wavelength-dependent absorption coefficients.

Several factors may contribute to the absence of undulations in the experimental data. For the SiNC data, the diameter variation along the SiNC axis across the laser spot is $\sim$100 nm, larger than the period of the undulations ($\sim$70 nm). Their absence could also be attributed to the fact that our laser excitation is not truly a plane wave of infinite extent. Despite their absence, we believe that the agreement using a fairly simple model is rather good, and that our model provides a reasonable description for the enhancement observed and its physical origin.

Strong size-dependent enhancement of the Raman scattering from uniform diameter and tapered silicon nanowires is shown to depend on d, λ_{laser}, complex optical index of refraction, and incident polarization state. Both incident and Raman-scattered light are strongly enhanced in the model description, resulting in an experimentally observed, total *RE* that approaches 3 orders of magnitude. The enhancement is explained in terms of the resonant scattering model, and good correspondence between the increase in the calculated and experimentally observed scattered intensity for decreasing diameter is obtained. Uniform and/or tapered nanowires produced with control of diameters and apex angles may permit rational design of functional nanostructured materials systems with control of the spectral and spatial EM scattering signatures. These results suggest conditions for more efficient coupling of radiation to Si and other indirect band-gap materials, thereby expanding opportunities for engineering the photonic and sensing properties of silicon and silicon-based nanostructures.

We thank Ari Sagiv, Zhorro Nikolov, Lemoda Laim, and Yu Zhang for technical assistance. J. S. acknowledges support from the Army Research Office (W911NF-04-100308), and from the Nano-Bio Interface Center (NSF-NSEC) at the University of Pennsylvania and Drexel University (DMR-0425780).

*To whom correspondence should be addressed.
Electronic address: spanier@drexel.edu

[1] N. L. Rosi and C. A. Mirkin, Chem. Rev. **105**, 1547 (2005).
[2] S. A. Maier *et al.*, Nat. Mater. **2**, 229 (2003).
[3] D. A. B. Miller, Proc. IEEE **88**, 728 (2000).
[4] L. Pavesi *et al.*, Nature (London) **408**, 440 (2000).
[5] H. Rong *et al.*, Nature (London) **433**, 292 (2005).
[6] O. Boyraz and B. Jalali, Opt. Express **12**, 5269 (2004).
[7] B. E. A. Saleh and M. C. Teich, *Fundamentals of Photonics* (John Wiley & Sons, New York, 1991).
[8] T. J. Kippenberg *et al.*, Opt. Lett. **29**, 1224 (2004).
[9] Q. Xu, V. R. Almeida, and M. Lipson, Opt. Lett. **30**, 35 (2005).
[10] H. Chew and D. S. Wang, Phys. Rev. Lett. **49**, 490 (1982).
[11] R. Ruppin, J. Opt. Soc. Am. A **15**, 1891 (1998).
[12] G. J. Rosasco and H. S. Bennett, J. Opt. Soc. Am. **68**, 1242 (1978).
[13] A. Ashkin and J. M. Dziedzic, Phys. Rev. Lett. **38**, 1351 (1977).
[14] M. Kerker, *The Scattering of Light and Other Electromagnetic Radiation* (Academic, New York, 1969).
[15] J. F. Owen *et al.*, Phys. Rev. Lett. **47**, 1075 (1981).
[16] D. K. Armani *et al.*, Nature (London) **421**, 925 (2003).
[17] F. M. Liu *et al.*, Chem. Phys. Lett. **382**, 502 (2003).
[18] D. V. Murphy and S. R. J. Brueck, Opt. Lett. **8**, 494 (1983).
[19] S. H. Zaidi, A. S. Chu, and S. R. J. Brueck, J. Appl. Phys. **80**, 6997 (1996).
[20] L. Y. Cao, L. Laim, C. Ni, B. Nabet, and J. E. Spanier, J. Am. Chem. Soc. **127**, 13 782 (2005).
[21] D. E. Aspnes and A. A. Studna, Phys. Rev. B **27**, 985 (1983).
[22] G. Mie, Ann. Phys. **25**, 377 (1908).